9. Sension, R. J.; Repinec, S. T.; Hochstrasser, R. M. *J. Chem. Phys.* **1990**, *93*, 9185.
10. Waldeck, D. H. *Chem. Rev.* **1991**, *91*, 415.
11. Goerner, H.; Schulte-Froehlinde, D. *J. Phys. Chem.* **1978**, *82*, 2653.
12. Goerner, H.; Schulte-Froehlinde, D. *J. Phys. Chem.* **1981**, *85*, 1835.
13. Mulliken, R. S.; Rppthaan, C. C. *J. Chem. Rev.* **1947**, *41*, 219.
14. Mulliken, R. S. *J. Phys. Chem.* **1977**, *66*, 2448.
15. Hans-Dieter Becker; kjell Andersson *J. Org. Chem.* **1983**, *48*, 4542.
16. Arai, T.; Karatsu, T.; Sakuragi, H.; Tokumaru, K. *Tetrahedron Lett.* **1983**, *24*, 2873.
17. (a) Karatsu, T.; Zeng, H.; Arai, T.; Sakuragi, H.; Tokumaru, K. *Chem. Phys. Lett.* **1985**, *115*, 9. (b) Arai, T.; Tokumaru, K. *Chem. Rev.* **1993**, *93*, 23-39.
18. Karatsu, T.; Kitamura, A.; Zeng, H.; Arai, T.; Sakuragi, H.; Tokumaru, K. *Chem. Lett.* **1992**, 2193.
19. Raj Gopal, V.; Mahipal Reddy, A.; Jayathirtha Rao, V. *J. Org. Chem* **1995**, *60*, 7966.
20. (a) Wadsworth, W. S. *Org React.* **1977**, *25*, 73. (b) Mahipal Reddy, A.; Raj Gopal, V.; Jayathirtha Rao, V. IUPAC conference, Bangalore, India. December 1994.
21. Lakowicz, J. R. In *Principles of Fluorescence Spectroscopy* Ed; Plenum press: New York, 1983; p 190.
22. Beer, M.; Longuet-Higgins, H. C. *J. Chem. Phys.* **1955**, *23*, 1390.
23. Morgante, C. G.; Struve, W. S. *Chem. Phys. Letters* **1979**, *687*, 267.
24. Hui, M. H.; Demayo, P.; Suau, R.; Ware, W. R. *Chem. Phys. Letters* **1975**, *31*, 257.
25. Hans-Dieter Becker; Hans-Christian Becker; Kjell Sandros; Kjell Andersson *Tetrahedron Letters* **1985**, *26*, 12, 1589.
26. Hans-Dieter Becker *Chem. Rev.* **1993**, *93*, 145.

Intramolecular Hydrogen Bonding Effect on the Excited-State Intramolecular Charge Transfer of *p*-Aminosalicylic Acid

Yanghee Kim and Minjoong Yoon*

Department of Chemistry, Chungnam National University, Taejon 305-764, Korea
Received June 13, 1998

The excited-state intramolecular proton transfer (ESIPT) emission has been observed for 0.01 mM *p*-aminosalicylic acid (AS) in nonpolar aprotic solvents as demonstrated by the large Stokes' shifted fluorescence emission around 440 nm in addition to the normal emission at 330 nm. However in aprotic polar solvent such as acetonitrile, the large Stokes' shifted emission band becomes broadened, indicating existence of another emission band originated from intramolecular charge transfer (ICT). It is noteworthy that in protic solvents such as methanol and ethanol the normal and ICT emissions are quenched as the AS concentration decreases, followed by the appearance of new emission at 380 nm. These results are interpreted in terms of ESIPT-coupled charge transfer in AS. Being consistent with these steady-state spectroscopic results, the picosecond time-resolved fluorescence study unravelled the decay dynamics of the ESIPT and ICT state *ca.* 300 ps and *ca.* 150 ps, respectively with *ca.* 40 ps for the relaxation time to form the ICT state.

Introduction

Aminosalicylate and its derivatives are well known molecules easily form the excited-state intramolecular proton transfer (ESIPT) through the intramolecular hydrogen bonding. For the first time, that was investigated by Kasha *et al.* several years ago. They suggested that some derivatives such as dialkylaminosalicylate form the triple fluorescence emission, normal locally excited-state emission, the proton transfer tautomer emission and the excited-state intramolecular charge transfer (ICT) emission which are in competitive with one another.[1,2] Especially, the third emission, the excited-state ICT emission can be controlled by many other factors, as revealed by a lot of reports for the excited-state ICT process which is a primary function for photoelectronic devices[3] as well as a basic mechanism of biological and chemical energy conversion.[4-7]

As an example of that factor, in some molecules, such as dimethylaminobenzonitrile (DMABN) derivatives, the excited ICT state formation followed by the solvent relaxation is important in determining the overall charge-transfer process.[8-12] Some other authors proposed that the photoinduced charge separation can be maximized by coupling with a conformational change of the electron donor group such as the twist of the whole alkylamino group which leads to a so-called "twist intramolecular charge transfer (TICT)" state[13,14] or the rehybridization of the nitrogen of the amino group, leads to the "wagged intramolecular charge transfer (WICT)" state.[15] Besides, according to recent HF/SCF and CIS calculations, bending

*Author to whom correspondence should be addressed.

of the cyano group, the electron acceptor group of DMABN is also considered to be followed by the twisting of the dimethylamino group.[16,17] The resulting "rehybridised ICT (RICT)" has been proposed to compete with the TICT mechanism in the ICT.

Also, the specific hydrogen bonding is an important factor to facilitate the ICT process by maintaining a large twist angle between the electron donor and the acceptor group in the ground state.[18] Such hydrogen bonding effect is an interesting subject to elucidate the proton-coupled charge transfer phenomenon which is often observed in biological assemblies including PS II systems.[19] In PS II the photoinduced charge separation is coupled to proton motion within quinone pool. The hydrogen-bonding effect has not attracted much attention, and Yoon *et al.* investigated the hydrogen-bonding effect on the ICT process by observing a change in the ICT emission of dimethylaminobenzoic acid (DMABA) upon adsorption of silica colloidal solutions or in aqueous cyclodextrin solutions.[20,21] From the observation of the change in the ICT emission of DMABA, they revealed that the intermolecular hydrogen bonding is very effective on the ICT process. However, the intramolecular hydrogen bonding effects on the ICT have not been considered yet.

Previously, Kasha *et al.*[1-2,22] have observed the excited-state intramolecular proton transfer (ESIPT) and the excited-state ICT for aminosalicylates, suggesting that ESIPT and the excited-state ICT are competitively occurred. Especially for AS, only ESIPT was observed. However, those results were obtained from a limited aprotic solvent system such as methylene chloride or cyclohexane. The limited solvent system does not provide full informations of the complex excited-state reactions including ICT and ESIPT. When one considers the ICT and ESIPT together, a specific solvent effect such as hydrogen bonding should be considered in addition to the long polarization effect. Thus, it is quite necessary to reinvestigate the photophysical properties of AS in protic polar solvents as well as in nonpolar solvents.

In this study, we attempted to explore the hydrogen bonding effects more systemically on the excited-state process of AS by observing the steady-state and time-resolved fluorescence spectral properties in various protic and aprotic solvents. Especially, in protic solvents, the concentration effects on the fluorescence spectral properties were also observed.

Experimental

Materials. *p*-Aminosalicylic acid (AS) was purchased from Aldrich Chemical Co.. It was purified by repeated recrystallization with ethanol until their melting points agree well with the reference values.[23] All the solvents were purchased from Merck. Chemical Co. as spectroscopic grade and used without further purification.

Spectroscopic Measurements. Absorption spectra were measured on a Varian Cary 3 Spectrophotometer. Steady-state fluorescence measurements were made on a scanning SLM-AMINCO 4800 spectrofluorometer which makes it possible to obtain corrected spectra using Rhodamine B as a quantum counter. The absorbance at the excitation wavelength was held constant when different solutions were compared. Fluorescence lifetimes were measured by a time-correlated single photon counting (TCSPC) method, using a dual-jet dye laser (coherent; model 702) synchronously pumped in a mode-locked Ar ion Laser (coherent; Innova 200) as described in a previous paper.[24] The cavity-dumped beam from the dye laser has 1 ps pulse width, average power *ca.* 100 mw at 3.8 MHz dumping rate, and a tunability of 560-620 nm with Rhodamine 6G as gain dye and DODCI (diethoxydicyanineiodide) as the saturable absorber. To excite the sample, the dye laser pulse was frequency-doubled using a β-BBO (β-barium borate) crystal. All the standard electronics used for the TCSPC were from EG & G Ortec. This method allows a time resolution of about 10 ps after deconvolution.

Results and Discussion

The absorption spectra of AS (0.01 mM) in various aprotic solvents, such as n-hexane, tetrahydrofurane (THF), ethylacetate (EA) and acetonitrile, shows two maxima, *ca.* 280 nm and *ca.* 300 nm. No change in spectral feature was observed upon changing the solvent polarity. However, the fluorescence spectra of AS (0.01 mM) was greatly changed by the solvent polarity. Figure 1 shows the fluorescence spectra measured in various aprotic polar and nonpolar solvents. These fluorescence spectra exhibit two emission bands at 330 nm and 440 nm which was originated from the local excited state and the relaxed excited state, respectively. Upon increasing the solvent polarity, the large Stokes' shifted emission band at 440 nm was quenched and broadened. Those behaviors are accompanied by an increase of the normal emission band at 330 nm. The large Stokes' shifted band was found to be separated into two bands, 430 nm and 470 nm by the band analysis using the gaussian distribution function (Figure 2). Further, the area ratio of 470 nm to 430 nm band was greatly enhanced by increasing the solvent polarity. As a result of this, the relaxed state should be composed of two different excited-states, and they are related to solvent polarity.

Figure 3 shows the absorption spectra of AS in ethanol containing different concentrations of AS. In protic solvents, such as methanol and ethanol the absorption spectra of AS

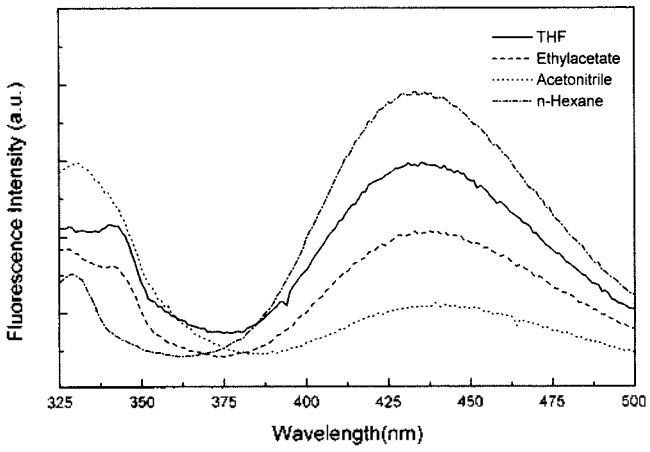

Figure 1. Fluorescence emission spectra of 1.0×10^{-5} M aminosalicylic acid in various aprotic solvents. The excitation wavelength is 300 nm.

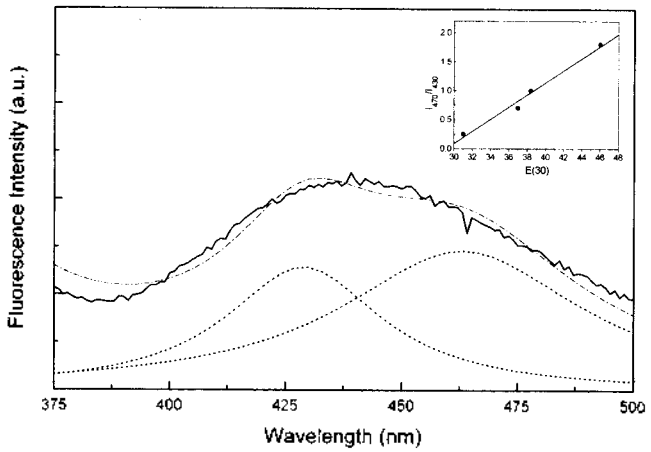

Figure 2. The band analysis of the Stokes' shifted emission of AS. The excitation wavelength is 300 nm. The inset is relative area ratio of the 470 nm emission band to the 430 nm emission band.

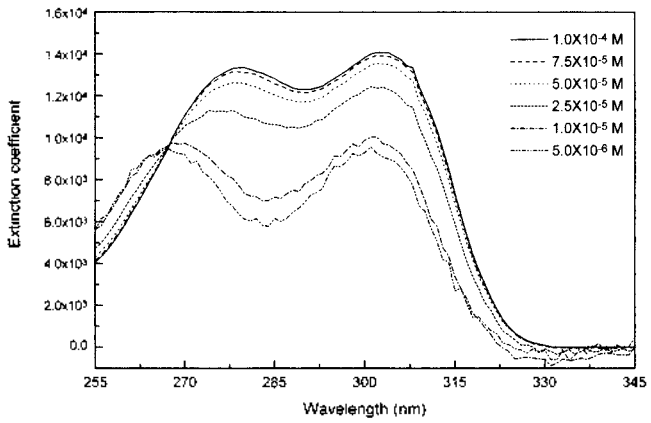

Figure 3. Absorption spectra of aminosalicylic acid in methanol as a function of concentration.

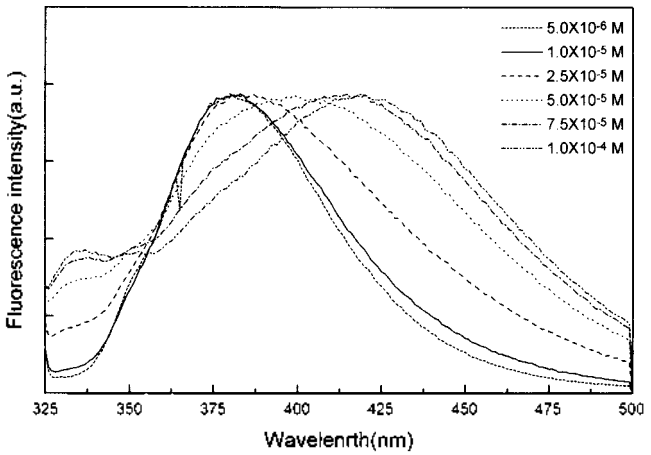

Figure 4. Fluorescence emission spectra of aminosalicylic acid in ethanol as a function of concentration. The excitation wavelength is 300 nm.

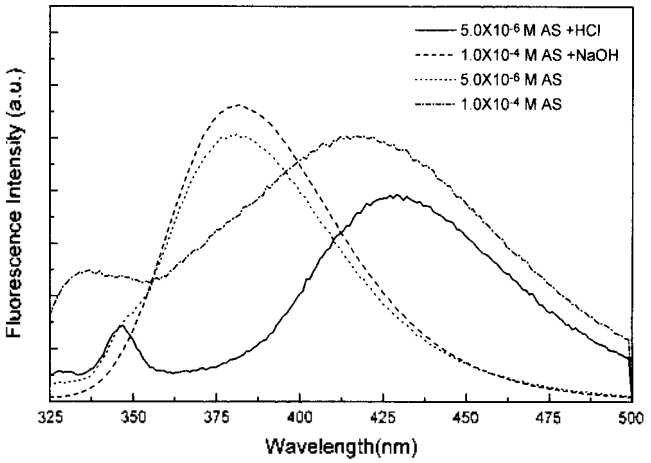

Figure 5. Acid-base dependent change in the fluorescence spectrum of AS in ethanol. The excitation wavelength is 300 nm.

were quite different from those observed in aprotic solvents.[1,2] The absorption spectra had two different maxima; the first one at 260 nm was gradually shifted to 280 nm with an appearance of isosbestic point at 270 nm by increasing the concentration of AS from 0.005 mM to 0.1 mM. However, as the result of the concentration dependent spectral shift, the absorption spectrum of 0.1 mM AS is in good match with that in measured aprotic solvents.[1,2] The fluorescence emission spectra observed in protic solvents were also greatly different from those observed in aprotic solvents (Figure 4). Only single fluorescence emission band was appeared at 380 nm in 0.005 mM ethanol solution. On the other hand, upon increasing the concentration, the fluorescence emission spectrum not only shifts to 420 nm but also represents dual emission band; one was 330 nm and the other was 420 nm. The dual emission of 0.1 mM AS in protic solvents was the same as that observed in aprotic solvents. However, in aprotic solvents, this type of spectral change was not observed by the change of concentration. For this reason, the concentration effects of AS in protic solvents seem to be basically caused by the specific interaction between AS and solvent molecules such as intermolecular hydrogen bonding. In order to confirm this, we attempted to observe the spectral change upon addition of acid and base to the protic solution. In case of the 0.005 mM AS in ethanol, the 380 nm emission band was shifted to 420 nm by the addition of acid, such as hydrochloric acid or acetic acid, while it was not changed by the addition of base, such as sodium hydroxide or triethylamine. The 420 nm emission band was shifted to 380 nm again by the addition of base in 0.1 mM AS solution (Figure 5) while it was not affected by addition of acid. The same result was obtained for the absorption spectra. These results indicate that the absorption and emission spectra observed in the dilute solution are originated from intermolecular hydrogen bonding species which forms an open conformer (conformer I) (scheme 1). However, an intramolecular hydrogen bonding is also accessible in AS molecule. Thus, the emission spectra observed in the concentrated solutions should be originated from the conformer II formed by intramolecular hydrogen bond as shown in Scheme 1, since they were the same as those observed in aprotic solvents. It should be also noted that the absorption and emission spectra measured in methanol-d were the same as those of the concentrated methanol solution without the concentration dependent spectral changes. This indicates that AS in the deuterated methanol

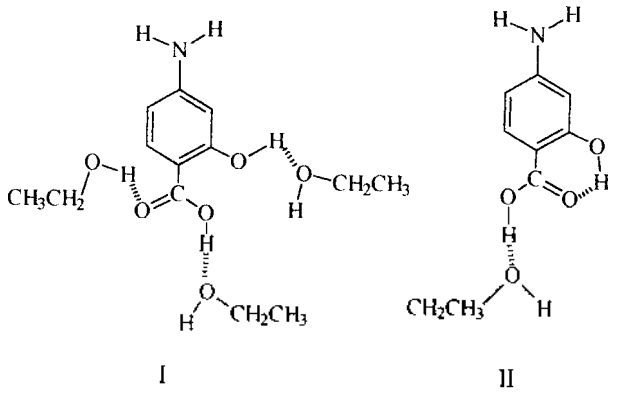

I II

Scheme 1

forms only one conformer which is originated from intramolecular hydrogen bonding.

Here it is noteworthy that fluorescence spectra observed in the concentrated protic solvents exhibit the dual emission at 330 nm and 440 nm corresponding to the normal and the relaxed state as in aprotic solvents. The large Stokes' shifted emission at 440 nm can be also analyzed into two bands as in aprotic solvents. These results again support the fact that the closed conformer II is dominant in the concentrated solution of protic solvents. Considering the fact that the area ratio of the analyzed band (470 nm/430 nm) of the large Stokes' shifted emission enhanced upon increasing solvent polarity as described above, an intramolecular charge transfer (ICT) as well as intramolecular proton transfer (IPT) is possible as the excited relaxation processes. Thus, the 470 nm emission is attributed to the ICT while the 430 nm emission is attributed to the ESIPT.

In order to confirm the interpretation of the steady-state emission, the fluorescence decay kinetics were investigated. Figure 6 shows the typical temporal profile of the large Stokes' shifted emission of AS in various aprotic solvents, exhibiting the fluorescence decay significantly affected by increasing the solvent polarity. The analyzed fluorescence decay times are summarized in Table 1. In nonpolar aprotic solvents, decay profile of the 430 nm emission is single exponential, and its decay time is within *ca.* 300 ps. As mentioned above, AS is known to easily form the ESIPT in

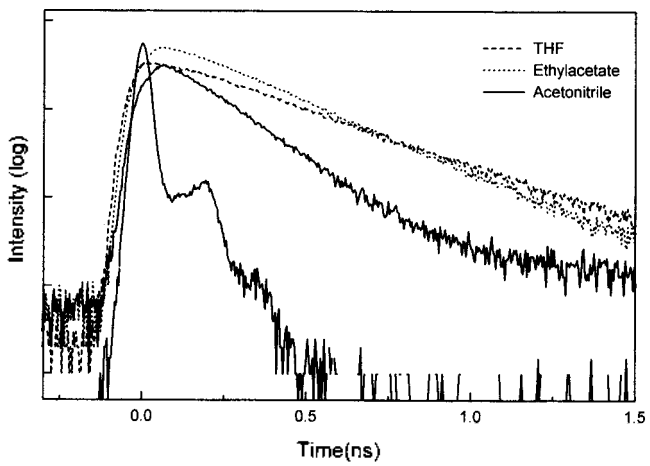

Figure 6. The fluorescence decay curve of aminosalicylic acid monitored at 430 nm. The excitation wavelength is 300 nm.

Table 1. Fluorescence lifetimes of AS in various aprotic solutions

solvent \ wavelength	430 nm	465 nm
THF	330 ps (1)	330 ps (1)
Ethylacetate	270 ps (0.85) 160 ps (0.15) rise time: 40 ps	280 ps (0.73) 150 ps (0.27) rise time: 40 ps
Acetonitrile	270 ps (0.09) 150 ps (0.91) rise time: 40 ps	270 ps (0.02) 150 ps (0.98) rise time: 40 ps

Excitation wavelength: 300 nm. Measurement error limits are less than 10% of the listed values.

aprotic solvents. Accordingly, the 300 ps component observed in nonpolar solvents such as n-hexane and THF should be originated from a tautomer formed from ESIPT process.[1] However, upon increasing the solvent polarity, the 430 nm emission decay curve exhibits a biexponential decay with two components, *ca.* 300 ps and *ca.* 150 ps. Also, the portion of *ca.* 150 ps is increased upon increasing the solvent polarity in contrast to that of 300 ps component. These results are different from the kinetics observed by Kasha *et al.* who suggested the existence of ESIPT state only in aprotic solvents.[1] This behavior is rather similar to the fluorescence decay of *p*-dimethylaminosalicylic acid methyl ester (DMASE), which is known to form the triple fluorescence emission indicating the normal, ESIPT and ICT emissions.[1,2] In aprotic polar solvents, the ratio of the normal locally excited-state emission to the Stokes' shifted emission of DMASE was greatly changed by increasing the solvent polarity.[1,2] These comparisons imply that the 150 ps decay component observed for AS in polar and nonpolar solvents should be originated from the excited ICT state. It is also noteworthy that a rise component (*ca.* 40 ps) is observed in polar solvents in contrast to its absence in nonpolar solvents. The rise time is too large to be the rate of ESIPT,[25] and its origin, we believe, is due to the forward conformational relaxation of excited AS followed by the polar solvent reorganization to facilitate the formation of the ICT state.

The previous work revealed that the hydrogen bonding plays an important role of the excited-state ICT.[20,21] Thus, the excited-state ICT in AS could be also coupled with the inter- and intramolecular hydrogen bonding. In order to certify this possibility, concentration effects on the fluorescence decay kinetics of AS in protic solvent such as ethanol were investigated. Figure 7 shows the typical temporal profile of the large Stokes' shifted band. The decay times observed in different concentration solutions are listed in Table 2. In the protic solvent, the decay kinetics were found to be affected by changing the concentration of AS. In case of the diluted ethanol solution (0.005 mM), the 500 ps component corresponding to the decay time of the ESIPT was observed with the appearance of new component *ca.* 1 ns. On the other hand, in the concentrated solution (0.1 mM), three different decay components could be observed, *i.e. ca.* 1 ns, *ca.* 300 ps and *ca.* 150 ps. The relative portion of the new component was

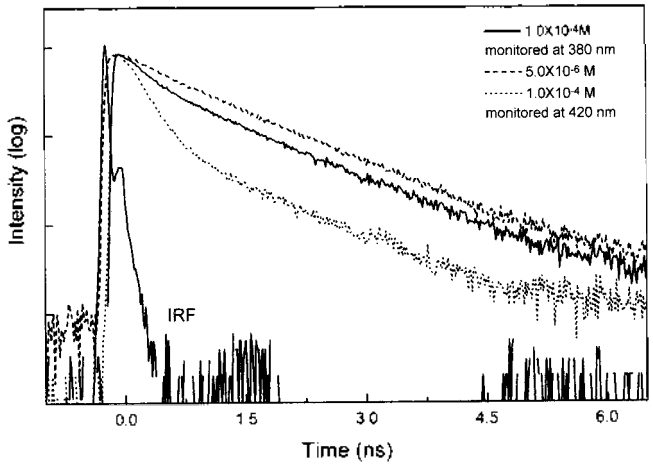

Figure 7. The fluorescence decay curve of aminosalicylic acid monitored at 380 nm and 420 nm. The excitation wavelength is 300 nm.

Table 2. Fluorescence lifetimes of AS in ethanol solutions

concentration of AS \ wavelength	380 nm	420 nm
1.0×10^{-4} M	1.14 ns (0.30)	1.16 ns (0.06)
	440 ps (0.22)	480 ps (0.02)
	150 ps (0.48)	220 ps (0.92)
	rise time: 45	rise time: 40
5.0×10^{-6} M	1.14 ns (0.79)	1.14 ns (0.75)
	500 ps (0.21)	420 ps (0.25)

Excitation wavelength: 300 nm. Measurement error limits are less than 10% of the listed values. The parenthesis represents the relative amplitude of each lifetime component.

much greater than that of 1 ns component measured in the concentrated solution. From the steady-state spectroscopic changes, the intermolecular hydrogen bonding was found to dominantly form in diluted protic solutions to form the open conformer I as shown in Scheme 1. Thus, the new decay component, (*ca.* 1 ns) should be originated from the open conformer formed by the intermolecular hydrogen bonding.[26]

However, these components of the 300 ps and 150 ps observed in the concentrated solution are similar to those observed in aprotic polar solvents. This indicates that the ICT state is easily formed in the concentrated protic solution as in aprotic polar solvents, in which the intramolecular hydrogen-bonding is facile to form the ESIPT state. If the ESIPT is competitive with ICT as proposed by Kasha *et al.*, the ICT emission could not be observed for AS in the aprotic polar solvents as described above. Therefore, the present results support that the ESIPT in aprotic polar solvent is prerequisite to form the ICT state as shown in Scheme 2. In nonpolar solvent, the energy of the excited ICT state (C*) is higher than that of ESIPT state (B*), and the ESIPT energy cannot be transferred to the ICT state.

In conclusion, the ICT is feasible when the closed conformer is formed by the intramolecular hydrogen-bonding. The theoretical calculation for the potential energy diagram is now in progress.

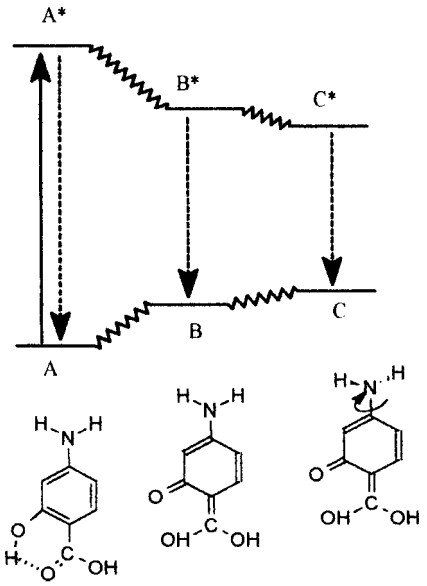

Scheme 2. Potential energy diagram of proton-transfer coupled ICT of AS.

Acknowledgment. This work has been financially supported by KOSEF through the Center for Molecular Catalysis at Seoul National University and the Basic Science Research Institute Program, Ministry of Education (BSRI-97-3432).

References

1. Heldt, D. Gomin; Kasha, M. *Chem. Phys.* **1989**, *136*, 321 and references therein.
2. Gormin, D.; Kasha, M. *Chem. Phys. Lett.* **1988**, *153*, 574.
3. Launay, J. P.; Sowinska, M.; Leydier, L.; Guaurdon, A.; Amouyal, E.; Boilot, M. L.; Heisel, F.; Miehe, J. A. *Chem. Phys. Lett.* **1989**, *160*, 89.
4. Khundkar, L. R.; Stiegman, A. E.; Perry, J. W. *J. Phys. Chem.* **1990**, *94*, 124.
5. Lueck, H.; Windsor, M.; Rettig, W. *J. Phys. Chem.* **1990**, *94*, 4550.
6. Retti, W.; Gleiter, M. *J. Phys. Chem.* **1985**, *89*, 4675.
7. Meech, S. R.; Phillips, D. *J. Chem. Soc. Faraday Trans.* **1987**, *2*, *83*, 1941.
8. Su, S. G.; Simon, J. D. *J. Chem. Phys.* **1988**, *89*, 908.
9. Su, S. G.; Simon, J. D. *J. Phys. Chem.* **1989**, *93*, 753.
10. Mataga, N.; Yao, H.; Okada, T.; Rettig, W. *J. Phys. Chem.* **1989**, *93*, 3383.
11. Simon, J. D.; Su, S. G. *J. phys. Chem.* **1989**, *92*, 2395.
12. Hicks, J.; Vandersall, M.; Babarogic, Z.; Eisenthal, K. E. *Chem. Phys. Lett.* **1985**, *116*, 18.
13. Rotiewicz, K.; Grellman, K. H.; Grabowski, Z. R.; *Chem. Phys. Lett.* **1973**, *19*, 315.
14. Rettig, W. *Angew. Chem. Int. Ed. Engl.* **1986**, *25*, 971.
15. Leinhos, U.; Kuhnle, W.; Zachariasse, K. A. *J. Phys. Chem.* **1981**, *95*, 2013.
16. Sobolesski, A. L.; Pomcke, W. *Chem. Phys. Lett.* **1996**, *250*, 428.
17. Sobolesski, A. L.; Pomcke, W. *Chem. Phys. Lett.* **1996**, *259*, 119.

18. Cazeau-Duroca, C.; Lyazidi, S. A.; Cambou, P.; Peirigua, A.; Cazeau, Ph.; Pesquer, M. *J. Phys. Chem.* **1989**, *93*, 2347.
19. Cukier, R. L. *J. Phys. Chem.* **1994**, *98*, 2377 and references therein.
20. Kim, Y.; Cheon, H. W.; Yoon, M.; Song, N. W.; Kim, D. *Chem. Phys. Lett.* **1997**, *264*, 673.
21. Kim, Y. H.; Cho, D. W.; Yoon, M.; Kim, D. *J. Phys. Chem.* **1996**, 100, 15670 and references therein.
22. Chou, Pi-Tai; Martinrz, M. L.; Cooper, W. C. *Chem. Phys. Lett.* **1992**, *198*, 188.
23. *The Merk Index of Chemicals and Drugs*, 12th Ed.; p 499.
24. Cho, D. W.; Kim, Y. H.; Kang, S. G.; Yoon, M.; Kim, D. *J. Phys. Chem.* **1994**, *98*, 558.
25. Shabestary, N.; EL-Bayoumi, M. A. *Chem. Phys. Lett.* **1984**, *106*, 107.
26. Joshi, H. C.; Mishra, H.; Tripathi, H. B. *J. Photochem. Photobiol.* **1997**, *105*, 15.

The Potential Energy Surfaces and Dipole Moment Functions of NH_2 by *ab initio* Effective Valence Shell Hamiltonian

Seung Hun Yun, YoungSok Yun, Jong Keun Park, and Hosung Sun*†

Department of Chemistry, Pusan National University, Pusan 609-735, Korea
†Department of Chemistry, SungKyunKwan University, Suwon 440-746 and Center for Molecular Science, KAIST, Taejon 305-701, Korea
Received June 26, 1998

The second order effective valence shell Hamiltonian (H^v), which is based on quasidegenerate many-body perturbation theory, is applied to determining the potential energy surfaces and the dipole moment functions of the various valence states of NH_2. The H^v calculated values are found to be in good agreement with those of other ab initio calculations or experiments. It signifies the fact that the H^v is a good *ab initio* method to describe the energies and properties of various valence states with a same chemical accuracy. Furthermore, it is shown that the lowest (second order for energy and the first order for property) order H^v method is very accurate for small molecules like NH_2 and the matrix elements of H^v which are computed only once are all we need to accurately describe all the valence states simultaneously.

Introduction

The quasidegenerate many-body perturbation theory (QDMBPT) is a Rayleigh-Schrödinger perturbation theory for quasidegenerate case. Here the quasidegeneracy means that states of interest are neither nondegenerate nor degenerate, rather the states lie very closely to each other in energy.[1-3] One of such quasidegeneracy may be found in valence electronic states of molecules. The effective valence shell Hamiltonian (H^v) theory is nonetheless the QDMBPT but the name comes from the fact that the quasidegenerate states are valence states. In H^v, the valence states are defined as states within valence space which is a small configuration state function space composed of prechosen valence orbitals. The reason why only valence space is considered in H^v is that the valence states are the most important states in chemistry. But the generality is not lost here because if one wants another states, say Rydberg states, one can easily expand the valence space to include whatever states of interest. The valence states in valence space may not be quasidegenerate. This problem is adequately solved in the effective valence shell Hamiltonian by giving a flexibility in defining the zeroth order Hamiltonian and molecular orbital energies. Therefore the H^v can be considered as the most rigorous quasidegenerate many-body perturbation theory.

H^v has been applied to various atoms,[4-6] many diatomics,[7-14] triatomics,[15,16] and polyenes.[17-22] Energy levels, excitation energies, ionization potentials, electron affinities, potential energy curves, transition dipole moments, oscillator strengths, and radiative transition probabilities are investigated using H^v.[7-14] For polyenes not only valence states but also Rydberg states as an example of intruder states are studied.[17-22] But for triatomics, except for the orbital structure change of BeH_2,[15,16] no applications of H^v have not been made yet.

In the present work we apply the second order H^v to determining the potential energy surfaces, relating quantities, and dipole moment functions of the valence states of NH_2. While several theoretical studies on NH_2 have been published,[23-31] not many experimental studies have been reported.[32-37] Among theoretical works Peyerimhoff *et al.*'s MRD-CI work is the most extensive so that it provides a good example to compare our H^v results with.[30] The purpose of the present work is to verify how well the effective valence shell Hamiltonian can reproduce the dipole properties as well as the valence state potential energy surfaces of triatomics with an example of NH_2. Therefore detailed analyses on the electronic structures of NH_2 are not presented, instead the focus lies on the nature